

FUNCTIONAL AND THERMAL 1D MODELING OF A REUSABLE LH2-TANK USING ECOSIM PRO/ESPSS AND COMPARISON TO CFD RESULTS

SPACE PROPULSION 2022

ESTORIL, PORTUGAL | 09 – 13 MAY 2022

Lukas Opp ⁽¹⁾, Henning Scheufler ⁽²⁾, Malte Stief ⁽³⁾, Jens Gerstmann ⁽⁴⁾

⁽¹⁾ German Aerospace Center (DLR), Bremen, Germany, Email: lukas.opp@dlr.de

⁽²⁾ German Aerospace Center (DLR), Bremen, Germany, Email: henning.scheufler@dlr.de

⁽³⁾ German Aerospace Center (DLR), Bremen, Germany, Email: malte.stief@dlr.de

⁽⁴⁾ German Aerospace Center (DLR), Bremen, Germany, Email: jens.gerstmann@dlr.de

KEYWORDS: propellant management, CALLISTO, liquid hydrogen, tank, reusability, thermal, functional, 1D modelling, CFD

ABSTRACT:

The CALLISTO reusable vertical take-off and vertical landing prototype vehicle (VTVL) is a joint project between CNES, DLR and JAXA.

In order to analyze the operational processes and thermal behavior at a system level within the scope of the liquid hydrogen tank of the CALLISTO vehicle, a 1D thermal and hydraulic model of the LH2 tank has been developed which is taking the thermal environment of the mission into account. The model features the capability to simulate the entire mission from initial tank chill down, propellant loading, boil-off venting and pressurization to post-flight residual propellant venting. This way the required propellant mass, boil-off rates and heat fluxes to the structure can be evaluated and their impact on the overall mission can be analyzed.

In order to correlate the effect of external forces on propellant sloshing but also to predict the pressurant budget and thermal residuals, data from dedicated CFD simulations has been used. The combination of multiple tools enables a more detailed understanding of all effects that have an impact on thermal and hydraulic behavior of the LH2 tank system during the mission. This paper compares both approaches, shows the advantages each has and their limits.

1. THE CALLISTO LAUNCH VEHICLE

Reusability and sustainability are getting more important in the space industry due to the growing drive towards lower launch costs and environmental awareness. In order to study and gain experience with reusable launch vehicles, the CALLISTO project was initiated in a trilateral collaboration of aerospace organisations between France led by CNES, Germany led by DLR and Japan led by JAXA. An overview of the project is presented in [1, 2 and 3]

For its flight campaigns, the demonstrator will launch from Kourou in French Guiana and subsequently return to the launch site to land. The maiden flight is planned for late 2024. A sketch of CALLISTO is shown in Fig. 1.

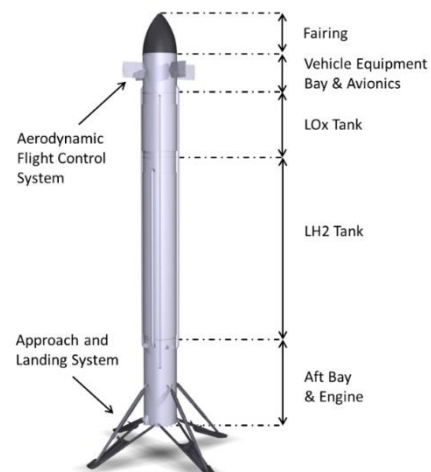


Figure 1. Callisto vehicle

The capability of reusability imposes certain requirements on the launcher and operations that do not need to be considered for traditional expendable launch vehicles. For the liquid hydrogen tank structure highly dynamic forces during re-entry, aero-thermodynamic loads, re-ignition of the engine (MEIG) and landing come into play. The fluidic aspects include additional propellant sloshing due to main engine cut-off (MECO) and possibly zero-G coasting phases or even negative acceleration. These would make propellant management devices such as tank baffles or propellant settling maneuvers prior to re-ignition of the main engine necessary.

In the case of sloshing, various effects occur that have an influence on the temperature distribution and the pressure in the tank. In the case of large sloshing movements, liquid boundary layers are mixed and the temperatures equalize. Parallel to this the free surface area increases and the

causes an increase in heat transfer between the gas and the liquid phase, leading to a cool down of the gas phase and thus a decrease in tank pressure. To counteract the pressure drop, more pressurant is needed. Additionally, condensation of GH2 into the liquid phase is triggered, which increases the thermal residuals while decreasing the tank pressure. However, evaporation of superheated droplets and additional wetting of the warmer tank walls cause the tank pressure to increase antagonizing the pressure drop effect described before. Consequently, the mean liquid temperature increases due to the mentioned effects, thus resulting in a higher thermal residual propellant mass.

Both CFD models use the volume of fluid method (VOF) to reconstruct the free surface with an additional conjugate heat transfer model implemented in the 2D axisymmetric model being capable of modeling phase change with multiple species utilizing the in house developed library *TwoPhaseFlow* [5,6].

The 2D model consists of the tank structure with a pressurization port at the top and a draining port at the bottom of the tank. Additionally, the insulating foam is considered. In contrast, the 3D model features a baffle configuration without consideration of the tank's metallic walls. Fig. 4 shows the tank domain with the baffle and the liquid surface undergoing a sloshing motion.



Figure 4. 3D-CFD model of the tank

The 2D CFD model, which is used in the following test case is discretized with ~120,000 / 35,000 (fine mesh / coarse mesh) elements in the fluid domain with an increased boundary layer resolution to account for boundary layer currents and heat transfer. Approximately ~280,000 elements are being used in the tank wall and ~470,000 elements in the insulation layer. Turbulence is not considered with the turbulence option set to laminar since an investigation revealed that turbulence models induce unrealistic currents at the free surface of the liquid.

The thermal environment consists of heat fluxes caused by natural convection during ground phases, aerothermal heat fluxes, solar radiation fluxes, infrared radiation within the engine bay and equipment compartments as well as heat conduction from the skirt's flanges.

4. DESCRIPTION OF THE TEST CASE

To compare the two models regarding their capabilities, a representative test case was created. The test case is limited to the flight phase, since this is the phase where propellant sloshing occurs and

therefore it is critical for the success of the mission to calculate pressurant usage and thermal residuals. Heat sources are limited to aerothermal heat loads, solar radiation, infrared radiation within the engine bay and equipment compartments and conductive heat loads from the skirt flanges. Both models are set up the same way by the following conditions with *T* indicating lift-off:

Start of Simulation	T - 0 s
End of Simulation	T + 238.4 s
Initial propellant mass	226.4 kg
Initial propellant temperature	20.5 K
Initial tank ullage pressure	2.8×10^5 Pa
Initial gas composition in ullage	
- Partial pressure of GH2	1.0×10^5 Pa
- Partial pressure of GHe	1.8×10^5 Pa
Initial ullage temperature	60 K
Tank pressure target during flight	2.8×10^5 Pa
GHe pressurization temperature	180 K
GH2 pressurization temperature	110 K

Table 1. Initial and boundary conditions

To pressurize the tank, a PID controller is used for the CFD simulation. In the 1D Simulation a fixed pressure boundary condition set to the tank target pressure is connected to the pressurization port. The gas used for pressurization is either GHe or GH2 depending on the flight phase and engine thrust level.

The thrust level over the mission with colored sectors indicating GH2 and GHe pressurization is shown in Fig. 5.

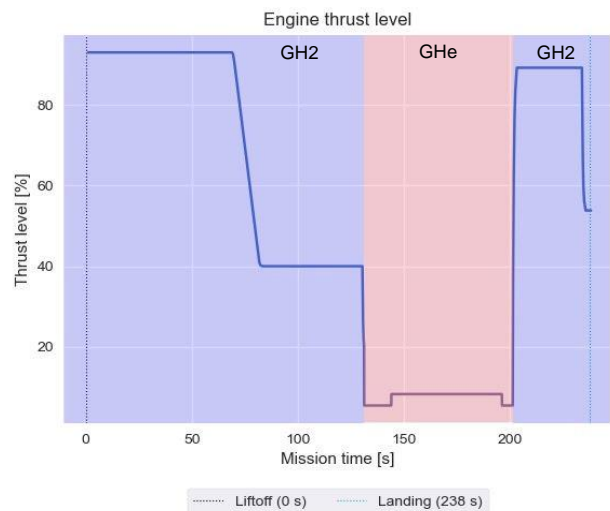


Figure 5. Thrust level over mission timeline

5. RESULTS

In this section, the results of the models are compared regarding tank ullage pressure, pressurization budget and thermal unusable mass. It took 35 hours to compute the 238 s long mission for the 1D model on an Intel Core i7-10850H processor. The CPU time for the CFD model was about 8 hours for the coarse mesh and 52 hours for the fine mesh on 32 cores using two AMD EPYC 7301 CPUs.

5.1. Tank pressure

The pressure evolution of the ullage during the mission is depicted in Fig. 6.

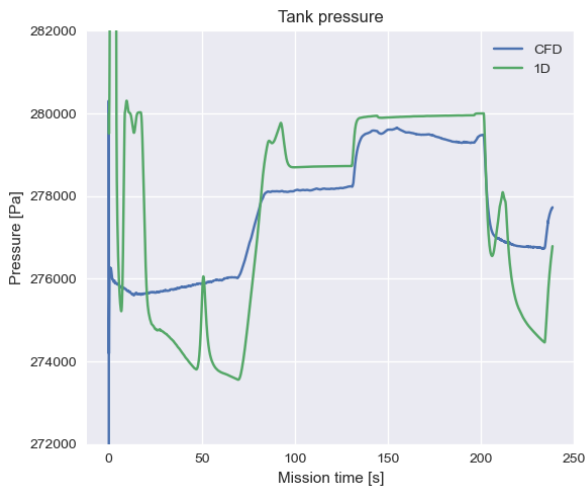


Figure 6. Tank ullage pressure

There is an initial spike in tank pressure observed in the 1D model reaching 336000 Pa, which is caused by imperfect initial temperature modeling of the tank wall causing a high evaporation mass flow in the liquid domain. Disregarding the initial transient of the 1D model, the pressure evolution is very similar between the two models. Since pressurization boundaries are modeled differently, a deviation in the tank pressure evolution is expected.

5.2. Pressurization budget

The pressurization budget is analyzed for GH2 and GHe pressurization. Fig. 7 shows the pressurization gas mass flow rate over mission time.

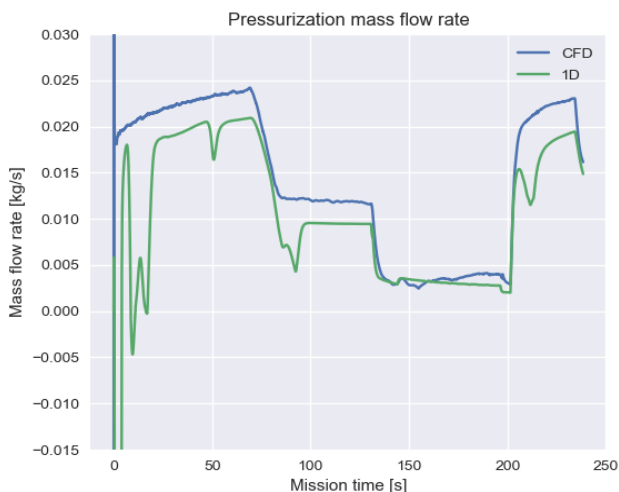


Figure 7. Pressurization mass flow rate

Disregarding the initial transient reaching -0.11 kg/s due to imperfect initial conditions, both models show a good agreement of the required pressurization mass flow rates. The 1D model shows a difference of the required GH2 mass of 46 % by integration of the mass flow rate compared to the CFD model. The difference in the pressurization mass flow rate,

especially in the propelled phases of the mission using GH2 as pressurant, is likely due to the boiling model causing spikes in the boiling mass flow rate at the beginning of the simulation but also later during the simulation, where occasional peaks in the boiling mass flow rate can be observed as shown in Fig. 8, causing an increase in tank pressure thus resulting in a dip in the pressurant mass flow rate.

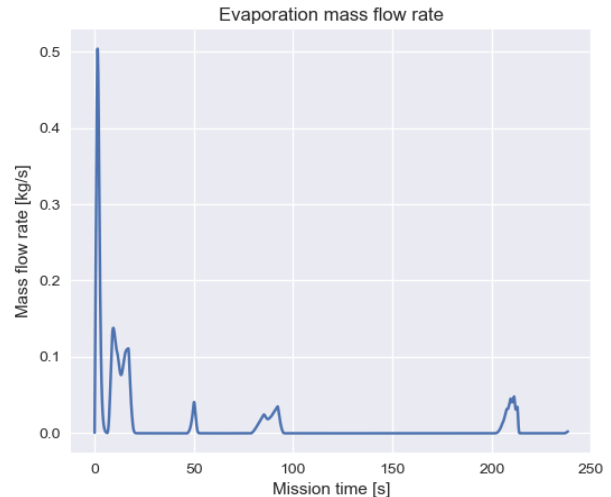


Figure 8. Evaporation mass flow rate

Another factor affecting the pressurant mass flow rate is a smaller diameter inlet port and an additional junction used in the 1D model causing a higher pressure drop across the pressurization port leading to a lower pressurization mass flow rate especially in phases where the pressurization flow velocity is higher. This effect becomes less prominent in engine off and idle phases, where a lower flow velocity of the pressurization gas is needed. Regarding the required GHe budget for engine idle and engine-off phases by integration of the mass flow rate over mission time, the models deviate by only 13 % with the 1D model calculating a lower pressurant mass compared to the CFD model. Here, both models are in better agreement than in the GH2 phases.

5.3. Thermal residual propellant mass

The thermal residual mass of the propellant is an important factor for the tank design. Therefore, a calculation is essential to avoid that liquid with an insufficient degree of subcooling becomes ingested by the turbo pumps which could cause cavitation if the pressure falls below the vapor pressure. Different CFD simulations using the 2D axisymmetric model based on the assumption of a sloshing Nusselt number [4] with and without the consideration of liquid sloshing visualize the effect of sloshing on thermal residuals. Here, the CFD model has a major advantage because of its ability to resolve the thermal boundary layer at the liquid / gas interface at any given time. Different CFD analysis (with and without sloshing) have been

carried out, comparing the temperature distribution of the residual propellant left inside the tank after landing. Sloshing is induced by the given trajectory causing partial decomposition of the free surface. It shows that the thermal boundary layer for the case without sloshing where the temperature of the LH2 exceeds a certain threshold has a thickness of just under 10 mm (Fig. 9) which lies outside of the capabilities of the coarser 1D model since subscale thermal gradients are smeared over the entire control volume.



Figure 9. Liquid temperature distribution without sloshing

Considering sloshing effects, the CFD model shows a thermal boundary layer of several centimeters at the time of the landing (Fig. 10), which would be resolvable with the 1D model due to the adaptive mesh causing a cell height reduction when the liquid column height decreases but consequentially cannot not resolve the thermal boundary layer for higher liquid column heights due to the smearing of the temperature gradient.

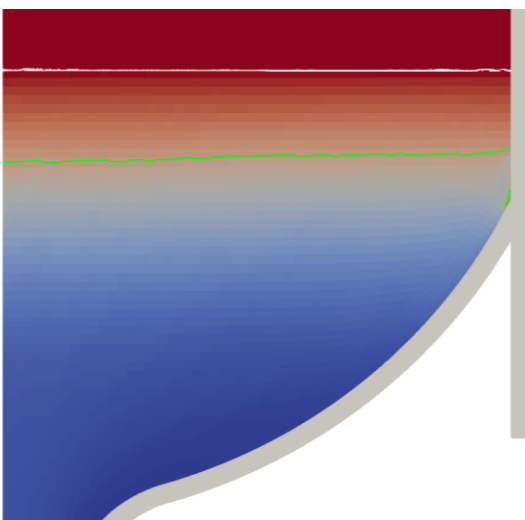


Figure 10. Liquid temperature distribution with sloshing (white line represents the free surface; green line represents the temperature threshold for the thermal unusable mass)

However, since the thicker thermal boundary layer is the result of sloshing effects, with the 1D model not being capable of capturing free surface effects, this increase of the thermal unusable mass is not present in the 1D model. Considering the limited number of control volumes in the 1D simulation, where one control volume has a height of 20 cm when the tank is completely filled at the beginning of the simulation, precise calculation of the stratification including the thermal boundary layer is not possible. A higher resolution of the grid would be necessary to precisely capture the stratification layer built up by buoyancy effects, however the increase of thermal residuals due to sloshing cannot be calculated with the current model.

6. CONCLUSION

A test case has been presented that allows for a comparison of both modeling approaches. It resembles a mission of the CALLISTO launcher. Several metrics as tank ullage pressure, pressurization budget and thermal residuals have been compared to show the advantages and limits of the proposed models.

Both models show a good agreement especially during engine off and idle phases where helium is used as pressurization gas. During propelled flight phases where hydrogen is used as the pressurant, the models show a larger discrepancy. Here, a modification of the initial conditions and also certain parameters of the wall boiling model used by the 1D model obtained by experimental data would reduce the deviation. Because of its substantially lower resolution, the thermal residual propellant mass cannot be calculated precisely with the 1D model since the thermal boundary layer is not resolved to an accuracy needed for such an assessment. The impact of increasing the discretization of the model by adding liquid and gaseous control volumes on computational time is enormous so that the 25 control volumes used in the liquid and gaseous phase respectively was the upper limit considering computational limitations and purpose of the model. The CFD model has an advantage over the 1D model when it comes to resolution and is able to resolve the thermal boundary layer so that the thermal residual mass can be calculated.

7. REFERENCES

1. Dumont, E., Ishimoto, S., Tatiassian, P., Klevanski, J., Reimann, B., Ecker, T., Witte, L., Riehmer, J., Sagliano, M., Giagkozoglou, S., Petkov, I., Rotärmel, W., Schwarz, R., Seelbinder, D., Markgraf, M., Sommer, J., Pfau, D. & Martens, H. (2021). CALLISTO: A Demonstrator for Reusable Launcher Key Technologies. Transactions of the Japan Society for Aeronautical and Space Sciences, Aerospace Technology Japan, 19 (1), Pages 106-115. JSASS doi: 10.2322/tastj.19.106. ISSN 1884-0485.

2. Ishimoto, S., Illig, M., Dumont, E. (2022). Development Status of CALLISTO. 33rd ISTS Conference, 28.Feb. – 4. Mar. 2022, Beppu, Japan.

3. Dumont, E., Ishimoto, S., Illig, M., Sagliano, M., Solari, M., Ecker, T., Martens, H., Krummen, S., Desmariaux, J., Saito, Y., Ertl, M., Klevanski, J., Reimann, B., Woicke, S., Schwarz, R., Seelbinder, D., Markgraf, M., Riehmer, J., Braun, B. & Aicher, M. (2022). CALLISTO: towards reusability of a rocket stage: current status. 33rd ISTS Conference, 28. Feb. - 4. Mar. 2022, Beppu, Japan.

4. Ludwig, C., Dreyer, M.E. & Hopfinger, E.J. (2013). Pressure variations in a cryogenic liquid storage tank subjected to periodic excitations. International Journal of Heat and Mass Transfer

5. Scheufler, H. <https://github.com/DLR-RY/TwoPhaseFlow>

6. Scheufler, H. & Roenby, J. (2021). TwoPhaseFlow: An OpenFOAM based framework for development of two phase flow solvers. arXiv:2103.00870